Journal of Hydraulic Research Vol. 48, No. 4 (2010), pp. 491–498
doi:10.1080/00221686.2010.492106

Research paper

Toe protection for spill-through and vertical-wall abutments

ANTÓNIO H. CARDOSO, *Department of Civil Engineering and Architecture, Instituto Superior Técnico, Av. Rovisco Pais, 1049-001 Lisboa, Portugal.*
Email: ahc@civil.ist.utl.pt

GONZALO SIMARRO, *Department of Civil Engineering, Universidad de Castilla – La Mancha, Av. Camilo José Cela s/n, 13071 Ciudad Real, Spain.*
Email: gonzalo.simarro@uclm.es (author for correspondence)

CRISTINA FAEL, *Department of Civil Engineering and Architecture, Universidade da Beira Interior, Edifício II das Engenharias, Calçada do Lameiro, 6200-001 Covilhã, Portugal.*
Email: cfael@ubi.pt

OLIVIER le DOUCEN, *Ecole Polytechnique Fédérale de Lausanne (EPFL), Laboratory of Hydraulic Constructions (LCH), Station 18, 1015 Lausanne, Switzerland.*
Email: olivier.ledoucen@epfl.ch

ANTON J. SCHLEISS, *Ecole Polytechnique Fédérale de Lausanne (EPFL), Laboratory of Hydraulic Constructions (LCH), Station 18, 1015 Lausanne, Switzerland.*
Email: anton.schleiss@epfl.ch

ABSTRACT
This study addresses the design of riprap aprons as a scour countermeasure near abutments under clear-water conditions. It deals with the lateral extent of riprap aprons and the geometry of the scour hole prevailing at the apron edge. The study applies to riprap aprons acting as granular filters. The scour depth appears to be independent for a sufficiently long relative abutment length. Scour holes develop farther away from spill-through abutments than from vertical-wall abutments; the distance between the point of maximum scour depth and the abutment increases with the relative abutment length. The effect of contraction on this distance was not identified. The angle defining the position of the deepest scour point is close to 30°. Neither the abutment shape nor the flow contraction seems to influence the minimum stable apron width.

Keywords: Abutment, clear water, experimentation, protection, riprap, scour

1 Introduction

A major cause for bridge foundation failure is scour. Consequently, the estimation of the scour characteristics and the design of scour countermeasures at bridge foundation elements continue to be a concern for hydraulic engineers (Radice *et al.* 2009, Muzzammil and Siddiqui 2009, Ghorbani and Kells 2008). Riprap mattresses are among the most popular scour countermeasures, where rock riprap is designed to create a physical barrier resisting the scour capacity of flow. Blocks can be placed directly on the approach flow embankment slopes or on the riverbed, around the toe of the abutment, to create a horizontal apron, sometimes termed launching apron.

According to Chiew (1995) or Melville *et al.* (2006), riprap aprons are prone to shear failure, edge failure, winnowing failure and bed-form undermining. Shear failure occurs where the individual riprap blocks are not heavy enough to resist entrainment by the flow; it is clearly linked to insufficient riprap block size. Winnowing consists of soil uplift from beneath the apron blocks; its intensity reduces as the apron thickness increases. Bed-form undermining is due to the movement of crests and troughs of bed forms (dunes or anti-dunes); this failure

Revision received 5 May 2010/Open for discussion until 28 February 2011.

ISSN 0022-1686 print/ISSN 1814-2079 online
http://www.informaworld.com

mechanism may occur in the main channel but is typically absent on flood plains. Edge failure occurs as riprap blocks fall into the scour hole that, though reduced in depth by the presence of a riprap apron, develops at its edge. It is assumed to occur if a row of blocks in the immediate vicinity of the abutment foundation fails. Undermining of the abutment foundation and slope failure of the abutment body may then be triggered.

Though failure modes are frequently interdependent, there is a reasonable consensus that: (i) shear failure may be mitigated through the specification of sufficiently large blocks, (ii) winnowing failure may be avoided by placing a synthetic or a natural filter beneath mattresses of appropriate thickness, (iii) bed-form undermining can be prevented by founding the apron at or below the level of the migrating bed-form troughs (Melville and Coleman 2000).

Edge failure may be avoided by a proper design of the apron plan configuration. The wider the apron, the farther away from the abutment the prevailing scour hole develops and the smaller are the scour hole dimensions and the probability of edge failure. For engineering purposes, the key issue then is the minimum apron width w assumed as apron plan dimension normal to the abutment perimeter (Fig. 1).

Systematic studies of riprap protection at bridge abutments started in the 1970s. Regarding the sizing of riprap blocks, the studies of Pagán-Ortiz (1991), Richardson and Davis (1995), Lagasse *et al.* (2001) and Melville *et al.* (2007), among others, contribute to the specification of stable median block diameter D_{r50} in the absence of failure modes other than shear failure, with D the diameter; r the riprap and the numerical subscript indicates percentage finer by weight. D_{r50} was related to the Froude number in the contracted cross-section. Cardoso and Fael (2009) and Cardoso *et al.* (2009) studied the effects of relative abutment length and abutment side slope to define the threshold approach flow intensity corresponding to the initiation of block dislodgement. From this value, the minimum size of stable blocks can be determined.

Apron thicknesses of the order of $2D_{r50}$, typically between D_{r100} and $3D_{r50}$, were suggested by Richardson and Davis (1995) or Melville and Coleman (2000) for blocks placed on synthetic or granular filters. Filters were recommended to prevent piping and winnowing of soil through the armor layer (e.g. Melville *et al.* 2006), a generally effective solution. On the contrary, in the absence of filters, the thickness of riprap mattresses to prevent winnowing may be impracticably high since failure may still occur even for thick riprap mattresses (Cardoso and Fael 2009). According to Melville *et al.* (2006), an alternative solution to riprap aprons is the extension of riprap right around the abutment and down to the expected scour depth. Partly due to construction difficulties and cost, this extension down to the total predicted scour depth is frequently not adopted and the riprap barely extends below the riverbed.

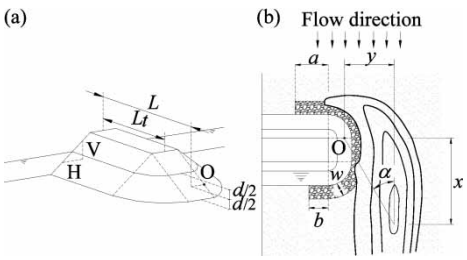

Figure 1 (a) Perspective and (b) schematic plan view of spill-through abutments

According to Richardson and Davis (1995), the extent of horizontal riprap aprons should be at least $w = 2d$, where d is the approach flow depth, but this ignores, for example, the effect of relative abutment length. Melville *et al.* (2006) reported an experimental study of scour countermeasures for spill-through abutments located in the flood plain. Its purpose was to determine the changes in the scour hole geometry by varying the compound channel and abutment geometries and to determine the width w of the toe riprap protection needed; predictors for engineering practice were suggested. Cardoso and Fael (2009) addressed the design of riprap aprons as a scour countermeasure near vertical-wall abutments, including their width w, and found that the predictor suggested by Melville *et al.* (2006) tends to be conservative, leading to rather wide aprons. However, both studies are not comparable since the abutment shapes considered are different and the experiments by Cardoso and Fael (2009) were carried out with blocks on a filter fabric that may have induced scale effects.

The present investigation concentrates on: (i) geometry of the scour hole prevailing at the apron edge and (ii) minimum width of riprap aprons to face edge failure, for both spill-through and vertical-wall abutments. The study investigated riprap aprons that act simultaneously as granular filters and have no underlaying filter fabric. Laboratory tests were carried out under clear-water flow conditions, i.e. conditions in which the mean undisturbed approach flow velocity is below or at the threshold velocity for entrainment of bed sediment. This choice is useful for the common situation encountered in floodplains where abutments are most frequently built.

2 Dimensional analysis

The required apron width w is assumed to be given as

$$w = \mathrm{f}\left(d, U, g, D_{r50}, D_{50}, \rho_s, \rho, \nu, L, s, B\right) \qquad (1)$$

where U is the mean approach flow velocity, g the gravity due to acceleration, ρ_s the riprap and sediment density, ρ the water density, ν the kinematic viscosity, L the abutment length, s the abutment side slope (H:V, where H means horizontal and V vertical; Fig. 1) and B the channel width. L of spill-through abutments is assumed to be defined at the mid-flow depth, whereas the vertical-wall abutment length $L = L_t$. The grain size distributions of the riprap and the bed sediment are assumed to be

uniform. Dimensional analysis yields

$$w^+ = \mathrm{f}\left(s_r, D_r^+, D_*, \mathsf{R}_s, \mathsf{F}, L^+, B^+, s\right), \tag{2}$$

where $s_r = \rho_s/\rho$ is specific gravity of blocks and sediment grains, and

$$D_r^+ = \frac{d}{D_{r50}}, \quad D_* = \frac{d}{D_{50}}, \quad \mathsf{R}_s = \sqrt{\frac{gD_{50}^3}{\nu^2}}, \quad \mathsf{F} = \frac{U}{\sqrt{gD_{50}}}, \quad L^+ = \frac{L}{d}, \quad B^+ = \frac{B}{L}, \quad w^+ = w/d. \tag{3}$$

According to Simarro *et al.* (2007), taking into account that the submergence ratio D_* is present in the control parameters and that sediment entrainment depends on the sediment characteristics that are accounted for, F can be replaced by the flow intensity parameter $I = U/U_c$ defined as the ratio of mean approach flow velocity to the critical velocity for bed sediment entrainment.

According to Fig. 1, the bed of the approach flow is composed of sand but the apron and the abutment side slopes are covered with rougher elements, i.e. riprap blocks. On top of that, the flow structure, including organized vortices, depends on the shape of the abutment, which constitutes a large roughness element. It can be reasonably assumed that, at least locally, the flow is turbulent rough. Viscous effects are negligible in this process and the effect of R_s may be discarded from Eq. (2). For constant s_r values, Eq. (2) reduces to

$$w^+ = \mathrm{f}\left(D_r^+, D_*, \mathsf{F}, L^+, B^+, s\right). \tag{4}$$

It seems also reasonable to assume that edge failure is not critically dependent on the size of the riprap blocks provided that they are heavy enough to resist horizontal-bed shear; they tend to fall into the prevailing scour hole irrespective of their size. Under this assumption, the effect of $D_r{}^+$ can also be ignored. Provided that the bed sediment size is much smaller than d and L, the flow structure does not depend on D_{50} and the effect of D_* vanishes. Nevertheless, D_{50} is accounted for by F (or the approach flow intensity I) of the approach flow. For constant F or constant I (with proper calculation of U_c to exclude the effect of viscosity), Eq. (4) reads

$$w^+ = \mathrm{f}\left(L^+, B^+, s\right), \tag{5}$$

where the effect of B^+ is negligible if $B^+ << 1$, i.e. if contraction effects are practically absent. The experimental campaign reported below was carried out for $I \approx 1$, to maximize both the depth of the prevailing scour hole and, this way, the probability of clear-water edge failure. Equation (5), therefore, constitutes the framework for the analysis. Note that similar reasoning would lead to the same set of independent dimensionless parameters for determining the geometry of the prevailing scour hole or the other characteristic dimensions of the riprap apron, namely its up- and downstream lengths a and b, respectively (Fig. 1).

3 Experimentation

Three horizontal-bed flumes were used herein, each including a central reach containing a recess box in the bed (Fig. 2), where the abutment models were placed, protruding at right angles from one of the vertical side walls. The main flume features are shown in Table 1, where Λ is the actual flume length (Fig. 2), λ the distance from flume entrance to abutment axis, Γ the length of bed recess box and δ its depth. The fix bed of the approach reaches was roughened with loose gravel to develop rough-bed boundary layers upstream the recess boxes.

Tests on spill-through abutments were carried out in flumes of Ecole Politechnique Fédérale de Lausanne (EPFL) and Universidad de Castilla, La Mancha (UCLM); abutment side slopes, H:V, were equal to 1:1 and 2:1. The spill-through abutments were impervious to water and roughened with a 7 mm thick layer of glued riprap; the height of the models measured from the surrounding bed and their top widths were 130 and 100 mm, respectively. Backwater did not induce overtopping. Tests on vertical-wall abutments were conducted in a flume of Universidade da Beira Interior (UBI). These were simulated using 140 mm wide, parallelepiped Perspex boxes with smooth vertical walls. All abutment models extended downwards vertically from the reference bed level so that their bases were directly placed on the floor of the recess boxes.

Five series of experiments, involving various combinations of B^+ and s, were performed (Table 2). Flow depth d was kept practically constant at 0.090 m in Series 1–4 and is equal to 0.120 m in Series 5. The abutment top length L_t varied between the limits listed in Table 2, at increments of 0.10 m, except for Series 5, where $L_t = L$ was equal to 0.30, 0.51, 0.72, 0.93 and 1.13 m, as reported by Cardoso and Fael (2009). Various sands were

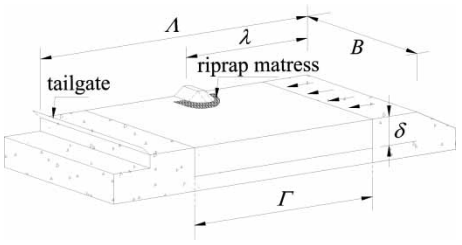

Figure 2 Sketch of longitudinal flume cross-section

Table 1 Main features of flumes

Flume	B (m)	Λ (m)	λ (m)	Γ (m)	δ (m)
EPFL	1.50	7.10	3.70	3.00	0.30
UCLM	3.00	7.00	3.60	4.00	0.60
UBI	4.00	28.0	15.4	3.0	0.60

Table 2 Characteristics of experimental series

					Riprap diameters (mm)				Sand diameters (mm)			
Series	B (m)	H:V	d (m)	L_t (m)	$D_{r15.9}$	D_{r50}	$D_{r84.1}$	σ_D	$D_{15.9}$	D_{50}	$D_{84.1}$	σ_D
1	1.50	2:1	0.09	0.20–0.30	6.1	7.0	8.1	1.2	0.71	0.96	1.25	1.3
2	1.50	1:1	0.09	0.10–0.50	6.1	7.0	8.1	1.2	0.71	0.96	1.25	1.3
3	3.00	2:1	0.09	0.30–0.60	6.1	7.0	8.1	1.2	0.87	1.19	1.68	1.4
4	3.00	1:1	0.09	0.10–0.50	6.1	7.0	8.1	1.2	0.87	1.19	1.68	1.4
5	4.00	0	0.12	0.30–1.13	13.4	15.7	18.7	1.2	0.87	1.28	1.87	1.5

used to fill the recess boxes. Riprap aprons of different plan sizes were embedded in the sand around the abutment nose, their top being level with the surrounding sand. The characteristic diameters of the riprap blocks used as apron material as well as of the sands are also reported in Table 2. Riprap blocks were identical in Series 1–4. Since $\sigma_D = 0.5(D_{84.1}/D_{50} + D_{50}/D_{15.9}) \leq 1.5$ for both sand and riprap mixtures, they can be assumed uniform.

For a given apron plan configuration, the volume of riprap stones was calculated by assuming a mattress thickness of $t = 3D_{r50}$, downstream apron length $b = 3D_{r50}$ and upstream apron length $a =$ minimum $\{L_t, 2d\}$. A thin flexible plate was inserted vertically in the sand bed along the external perimeter of the idealized apron, and the same sand volume was carefully removed from the space that the stones were to fill. For Series 1–4, the calculated riprap volume was finally poured into the excavated sand bed, to guarantee the same top level as the surrounding sand bed. Since riprap blocks were verified to act as granular filters, winnowing failure was mitigated. For Series 5, riprap blocks did not conform to the criteria of Terzaghi–Vicksburg for granular filters, since $D_{r15}/D_{85} \approx 7.2 > 5$; consequently, in this series, the lower one-third of the riprap aprons was replaced by a granular filter composed of finer riprap blocks ($D_{r50} = 7.5$ mm, $\sigma_D = 1.44$), to also inhibit winnowing failure. This procedure contrasts with that reported by Cardoso and Fael (2009), where a filter fabric was placed beneath the blocks to avoid winnowing in otherwise similar tests. In all tests, a row of yellow painted stones was carefully hand-placed around the abutment perimeter (white strip around abutment in Fig. 3a).

Once the abutment, sand bed and riprap apron were placed, the flumes were slowly filled with water up to a certain flow depth. To avoid disrupting the bed and apron, the discharge was slowly increased up to the test value and flow depth was simultaneously adjusted. The discharge Q was measured using electromagnetic flow-meters at EPFL and UBI and using a triangular thin-plate weir at the UCLM flume. The flow depths were regulated by hand-operated tailgates at the downstream flume end. Tests were carried out for $U \cong U_c$, namely for $0.95U_c < U < U_c$, in which U_c was computed by Neill (1967). Approximate values of Q were 40 l/s at EPFL, 90 l/s at UCLM and 160 l/s at UBI. Riprap blocks were much heavier than sand grains and shear failure never occurred. Bed-form undermining also did not occur since, in the absence of bed particles motion, bed forms could not develop, such that only edge failure developed.

Since armouring aprons tend to divert scour holes from abutments reducing the scour depth, it was assumed that edge failure occurred if at least one yellow painted block was dislodged from its original position and had fallen into the scour hole (Fig. 3b). Experiments were continued until failure was observed or equilibrium scour depth was reached. To identify the equilibrium stage, the scour hole depth was measured regularly with an adapted point gauge and plotted in a semi-logarithmic time scale, until a quasi-horizontal plateau was observed, as suggested by Cardoso and Bettess (1999).

4 Results and discussion

4.1 *Data presentation and characterization*

For a given abutment length, at least two values of apron width w were tested, yet only the results pertaining to the wider failing ("incipient" failure) and the narrower stable apron are discussed.

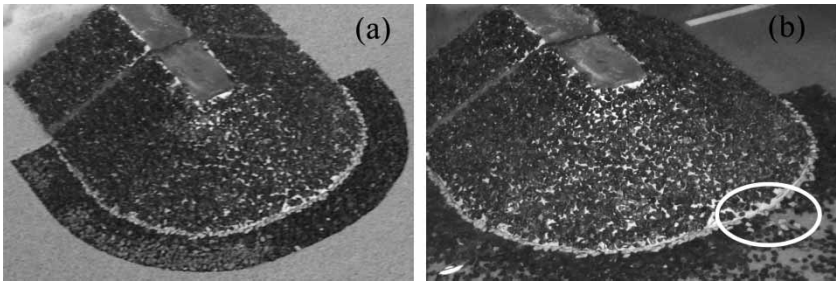

Figure 3 Apron configuration (a) before a test and (b) after a failure test

The complete data of Cardoso and Fael (2009) on vertical-wall abutments are also included in the analysis; as stated above, these refer to tests where a filter fabric was placed below the riprap apron and are available at http://www.uclm.es/profesorado/gsimarro/doc/papers/p080715_data.doc. The data include values of L_t, w and d as well as test duration T, maximum scour depth d_s, corresponding to the equilibrium scour depth whenever edge failure did not occur, the streamwise and cross-wise plan coordinates of the deepest scour hole points x and y, as defined from the origin O (Fig. 1), and information on whether incipient failure was observed or the tests corresponded to the narrowest stable width for a given geometry. The data cover values of $D_r^+ = 12.9$ for Series 1–4, 7.6 for Series 5, and the data by Cardoso and Fael (2009), except for Series 3 and 4, where $D_* = 75.6$ and $D_* = 93.8$, confirming the hypothesis of Eq. (5). L^+ ranged between 2.1 and 9.4, while $B^+ \leq 0.39$. Note that the average duration of equilibrium apron tests was 7 days; tests in which failure occurred were slightly shorter, lasting 5.2 days in the average (between 19 and 329 h). The values of $L \neq L_t$ for spill-through abutments and of the dimensionless parameters L^+, $d_s^+ = d_s/d$, $x^+ = x/d$, $y^+ = y/d$, w^+ and $\alpha = \arctan(y/x)$ were also recorded, as they represent important properties of the scour holes.

4.2 *Geometrical properties of scour holes*

To characterize equilibrium scour holes, only data corresponding to stable aprons were retained. Figure 4 shows the variation of d_s^+ with L^+. The data can be divided into two groups, corresponding to vertical-wall ($s = 0$) and spill-through abutments ($s = 1, 2$), respectively. In both groups, d_s^+ seems to be independent of L^+ if $L^+ > \approx 6$, since the behaviour begins to oscillate. This limit is smaller than the corresponding value for unprotected abutments, which is ≈25 (Melville 1997). This requires a confirmation for a wider range of L^+. Within the group of spill-through abutments, it is not possible to clearly distinguish the variation of equilibrium scour depth with abutment side slope. At best, one concludes that for milder slopes (Series 1 and 3) the data tend to plot higher than those for steeper slope (Series 2 and 4), contradictory to expectations. Still, this may be derived from the fact

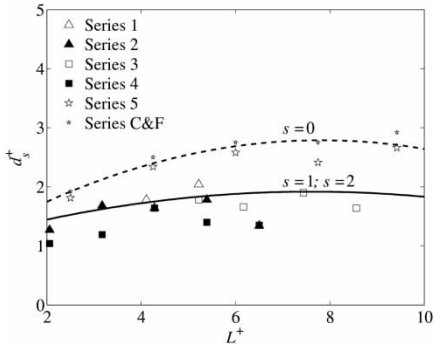

Figure 4 Variation of d_s^+ with L^+ for various side slopes and flow contractions

that $s = 2$ determines a larger flow contraction near the bottom. A close look at Fig. 4 indicates that there exists a small but systematic contraction effect on the scour depth, since the data of Series 1 and 2 are higher than those of Series 3 and 4.

Figure 5 shows the variation of x^+ and y^+ with L^+, including (a) the regression parabolas fitted to the data grouped into $s = 0$ and $s = (1, 2)$ and (b) focusing on data from Series 2 and 4, where contraction is the main difference. It can be concluded that (i) x^+ and y^+ are slightly larger for spill-through than for vertical-wall abutments, (ii) in contrast to d_s^+, x^+ and y^+ seem to increase with L^+, within the entire experimental range, (iii) contraction does not seem to influence x^+ and y^+ (Fig. 5(b)). The apparent decrease in y^+ with L^+ for $L^+ > 6$ at vertical-wall abutments ($s = 0$) is forced by few oscillating points and a parabolic-type fitting, but should not be regarded as a physical trend. The trends for $L^+ < 6$ are essentially linear. Conclusion (i) reflects the origin definition of the axes and must be regarded with caution; conclusion (ii) can be explained since the longer the abutment, the more it diverts the intercepted flow towards the flume centre.

According to Melville *et al.* (2006), the distance between the maximum scour hole depth and the abutment is

$$R^+ = 4\left(L^+\right)^{0.2}\left(1 + w^+\right)^{0.4}, \tag{6}$$

where $R^+ = R/d$ and $R = (x^2 + y^2)^{0.5}$. The deviation between observations and predictions is (2.05 ± 11.5)%. Despite the important scatter induced by the present abutment types, Eq. (6) constitutes a reliable predictor for R. From the data, $\alpha = (29.34 \pm 3.9)^o$ (average ± standard deviation). This compares well with $(30.6 \pm 2.9)^o$ of Cardoso and Fael (2009) and agrees with Melville *et al.* (2006). Figure 6 shows the variation of "stable" α with L^+. The slope of the inclined straight line is 1.30 and its 95% confidence interval is [0.78; 1.83], indicating the dependence of α on L^+. In spite of the significant scatter, α increases with L^+ while the effects of s and B^+ cannot be identified.

4.3 *Minimum apron plan dimensions*

From a practical point of view, the most important results reported refer to w, derived from the narrower stable and the wider failing tests, to identify the failure limit. Their non-dimensional form $w^+ = w/d$ are plotted against L^+ in Fig. 7. An effect of different geometries is absent since the data do not allow to identify any systematic variation of w^+ neither with s nor with B^+. This is consistent with the fact that the equilibrium scour hole geometry is only slightly influenced by contraction (Figs 4 and 5). For $L^+ > 6$, there seems to be a trend for w^+ (both wider failing and the narrower stable) to become constant, reflecting the invariance of d_s^+, but this is less pronounced than for d_s^+ and deserves further investigation.

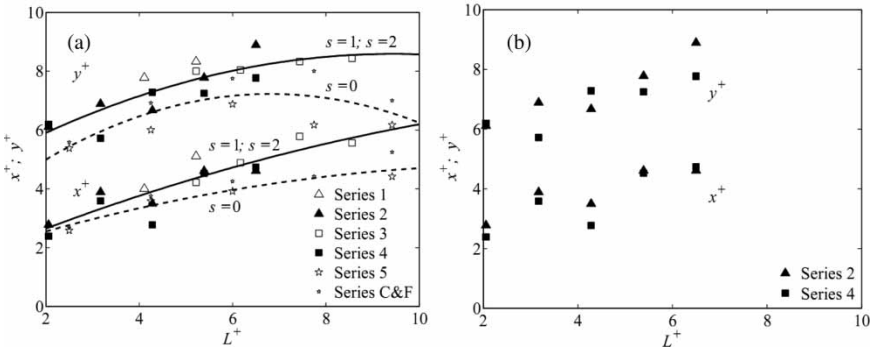

Figure 5 Variation of x^+ and y^+ with L^+ for (a) different side slopes and (b) different flow contractions

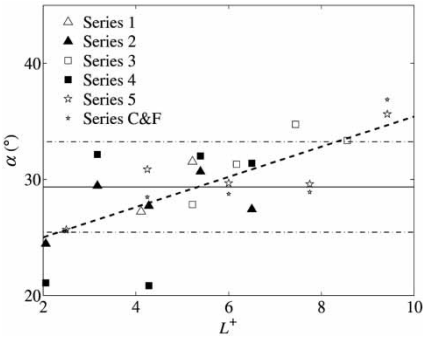

Figure 6 Variation of α with L^+ for stable aprons

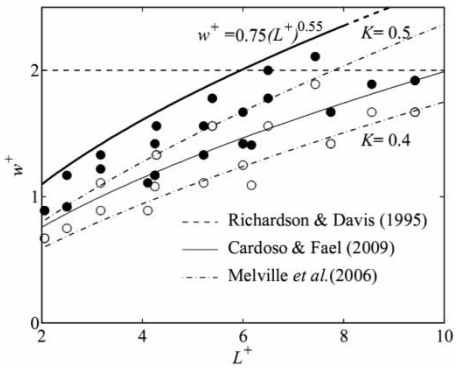

Figure 7 Variation of lateral extent of riprap apron w with L^+. Black symbols refer to narrower stable tests, white symbols to wider failure

Figure 7 also assesses the applicability of existing w predictors, namely those of Richardson and Davis (1995), Melville *et al.* (2006) and Cardoso and Fael (2009). Richardson and Davis' predictor simply reads $w^+ = 2$. According to Cardoso and Fael (2009), the minimum lateral extent of stable riprap aprons is

$$w^+ = 0.5\left(L^+\right)^{0.6}, \tag{7}$$

while the predictor of Melville *et al.* (2006) reads

$$w^+ = 0.5\left(d_s^+\right)^{1.35}, \quad \text{with} \quad d_s^+ = 2K\left(L^+\right)^{0.5}, \tag{8}$$

where K the shape factor $= 1$ for vertical-wall abutments. The value of K was taken as 0.4 and 0.5 for spill-through abutments with side slopes of $s = 2$ and $s = 1$, respectively. From Fig. 7, it can be concluded that though not adhering to observations for $L^+ < \sim 6$, the predictor of Richardson and Davis (1995) almost systematically renders safe w^+ values. In contrast, the predictors of Melville *et al.* (2006) and Cardoso and Fael (2009) follow the same trend as the data but tend to under-predict w^+. The differences between the predictor of Melville *et al.* (2006) may originate from a different experimentation.

Note that for $K = 1$, w^+ predictions by Melville *et al.* (2006) were verified to be exaggerated. Since (i) the safety of the predictor of Richardson and Davis (1995) necessarily conflicts with economy, (ii) the predictor of Cardoso and Fael (2009) based on limited experimental evidence may be unsafe, and (iii) the predictor of Melville *et al.* (2006) seems unnecessarily linked with the correct prediction of the scour depth, a new predictor is proposed as

$$w^+ = 0.75\left(L^+\right)^{0.55} \tag{9}$$

constituting an envelope curve to the w data for stable aprons (Fig. 7). The above expression can also be used for wire crated or cable-tied blocks, yielding results on the safety side, since Eq. (9) has been obtained from less favourable conditions.

It should finally be stressed that though no systematic evaluation of a and b was performed herein, there was sufficient evidence in the reported experiments that for (i) $b = 3D_{r50}$ can be taken as $b = 0$ without risk of edge failure and (ii) $a =$ minimum $\{L_t, 2d\}$ was frequently observed to nearly produce edge scour, particularly if $L_t > 2d$.

5 Conclusions

This study concentrates on the definition of the geometry of scour holes prevailing at the edge of abutment aprons and on their minimum stable width, for both spill-through and vertical-wall abutments. The main conclusions are as follows.

- Scour-depth data split into two groups, corresponding to

vertical-wall and spill-through abutments, respectively, reflecting abutment shape; scour depth appears to become independent of the relative abutment length if this variable is higher than 6 but this deserves confirmation.

- Scour holes seem to develop farther away from spill-through than from vertical-wall abutments; the distance between their deepest point and the abutment increases with the relative abutment length. In contrast, the influence of contraction on this distance could not be identified; the angle defining the position of the deepest scour hole point is close to 30° for practical purposes.
- Neither abutment shape nor flow contraction seems to affect the minimum stable apron width; the apron width tends to become independent of the relative abutment length for values of this non-dimensional parameter higher than 6 but this deserves also further research. The simple predictor of Richardson and Davis (1995) provides safe predictions of the minimum apron width, but may largely over-predict this variable for small relative abutment lengths; both the predictors of Melville *et al.* (2006) and Cardoso and Fael (2009) tend to under-predict the minimum safe width for spill-through abutments. A new predictor of the minimum safe apron width is proposed.

Acknowledgements

Ecole Polytechnique Fédérale de Lausanne, Universidad de Castilla – La Mancha, and the Portuguese Foundation for Science and Technology are acknowledged for supporting the first author to perform experiments. The authors also thank Eduardo Díaz for preparing the tests at UCLM.

Notation

a = upstream apron length
B = channel width
b = downstream apron length
D_n = characteristic diameter of bed sand such that n% by weight is finer
D_r^+ = inverse of relative riprap roughness
D_* = inverse of relative sand roughness
d = flow depth
d_s = maximum scour depth
F = sediment Froude number
g = acceleration due to gravity
I = flow intensity
K = abutment shape factor
L = abutment length
L_t = abutment top length
R = distance from deepest point of scour hole to abutment
R_s = sediment Reynolds number
s = abutment side slope
s_r = specific gravity of riprap blocks and sediment grains
T = test duration
t = mattress thickness
U = average flow velocity
U_c = critical flow velocity for sediment entrainment
x = stream-wise coordinate of deepest scour point
y = cross-wise coordinate of deepest scour point
w = apron width
α = angle defining position of deepest scour point
Γ = length of bed recess box at flume bed
δ = depth of recess box at flume bed
Λ = flume length
λ = distance from flume entrance to abutment axis
ν = kinematic viscosity of water
ρ = density of water
ρ_s = riprap and sediment density
σ_D = gradation coefficient of riprap blocks or bed material

Superscripts

$+$ = non-dimensional parameter

References

Cardoso, A.H., Bettess, E. (1999). Time evolution and effect of channel geometry on local scour at bridge abutments. *J. Hydraulic Engng*. 125(4), 388–399.

Cardoso, A.H., Fael, C.M.S. (2009). Protecting vertical-wall abutments with riprap-mattresses. *J. Hydraulic Engng*. 135(6), 457–465.

Cardoso, A.H., Simarro, G., Le Doucen, O., Schleiss, A. (2009). Sizing of riprap for spill-through abutments. *J. ICE Water Manage*, doi: 10.1680/wama.900024.

Chiew, Y.M. (1995). Mechanics of riprap failure at bridge piers. *J. Hydraulic Engng*. 121(9), 635–643.

Ghorbani, B., Kells, J.A. (2008). Effect of submerged vanes on the scour occurring at a cylindrical pier. *J. Hydraulic Res*. 46(5), 610–619.

Lagasse, P.F., Zevenbergen, L.W., Schall, J.D., Cloper, P.E. (2001). *Bridge scour and stream stability countermeasures*. Hydraulic Engineering Circular 23 (HEC-23). Report FHWA-NH1-01-003. Federal Highway Administration, Washington, DC.

Melville, B.W. (1997). Pier and abutment scour: integrated approach. *J. Hydraulic Engng*. 123(2), 125–136.

Melville, B., Ballegooy, S., Coleman, S., Barkdoll, B. (2006). Countermeasure toe protection at spill-through abutments. *J. Hydraulic. Engng*. 132(3), 235–245.

Melville, B., Ballegooy, S., Coleman, S., Barkdoll, B. (2007). Riprap size selection at wing-wall abutments. *J. Hydraulic Engng*. 133(11), 1265–1269.

Melville, B., Coleman, S. (2000). *Bridge scour*. Water Resources Publications, Fort Collins, CO.

Muzzammil, M., Siddiqui, N.A. (2009). A reliability-based assessment of bridge pier scour in non-uniform sediments. *J. Hydraulic Res*. 47(3), 372–380.

Neill, C.R. (1967). Mean velocity criterion for scour of coarse uniform bed-material. Proc. 12th *IAHR Congress*, Fort Collins, CO, 3(C6), 1–9.

Pagán-Ortiz, J.E. (1991). *Stability of rock riprap for protection at the toe abutments located at the floodplain*, Federal Highway Administration Research Report FHWA-RD-91-057. US Department of Transportation, Washington, DC.

Radice, A., Ballio, F., Porta, G. (2009). Local scour at a trapezoidal abutment: Sediment motion pattern. *J. Hydraulic Res*. 47(2), 250–262.

Richardson, E.V., Davis, S.R. (1995). *Evaluating scour at bridges*, Hydraulic Engineering Circular 18 (HEC-18). Report FHWA-IP-90-017: 204. Federal Highway Administration, Washington, DC.

Simarro, G., Teixeira, L., Cardoso, A.H. (2007). Flow intensity parameter in pier scour experiments. *J. Hydraulic Engng*. 133(11), 1261–1264.